XL CILAMCE
IBERO-LATIN AMERICAN CONGRESS ON COMPUTATIONAL METHODS IN ENGINEERING
NOVEMBER 11-14, 2019
Praiamar Natal Hotel & Convention Natal, RN-BRAZIL

DYNAMIC ANALYSIS OF PLANE STRESS PROBLEMS BY THE HIERARCHICAL FINITE ELEMENT METHOD WITH THE USE OF ERROR INDICATORS FOR SELECTIVE MESH ENRICHMENTS

Carolina C. Cittadin
Marcos Arndt
carolinacittadin@gmail.com
arndt.marcos@gmail.com
Graduate Program in Civil Construction Engineering, Federal University of Paraná
Centro Politécnico - UFPR, 81531-980, Paraná, Brasil

Abstract. The search for optimized projects has led to the design of leaner and lighter structures, which are more susceptible to dynamic effects. These must be thoroughly analyzed in order to avoid excessive displacements, structural damage and to guarantee user comfort. However, the analytic solution of dynamic problems tends to present great difficulties and, in some cases, cannot be obtained. Therefore, researchers developed approximated methods. The most used approximated method is the Finite Element Method (FEM). As a well-established method, the main focus of FEM studies has shifted from the development of the method to the improvement of its results. In this context two lines of research have proven to greatly influence the accuracy and efficiency of the method, the study of refinements and the study of error indicators. Even though refinements improve the accuracy of solutions they can lead to greater computational efforts and complexity. A way to balance these drawbacks is to combine them with error indicators. These allow the engineer to specify which mesh elements have greater influence on the results and apply refinements selectively. The present study focuses on precisely these characteristics and evaluates the use of the Friberg Error Indicator in the dynamic analyses of two-dimensional structures as a mean to the application of a selective *p*-refinement. Numerical examples, considering plane stress state, are computationally modeled with the use of Lobatto's hierarchical shape functions and trigonometrical enrichments. The results of eigenvalues for the enrichment of different elements are compared with those present in past literature.

Keywords: Finite element method, Selective mesh refinement, Friberg indicator

1 Introduction

The importance of dynamic analysis is many times associated with extreme loading scenarios such as those created by earthquakes. However, if the direction, orientation or magnitude of a load changes over time it will have a dynamic effect on the structure it acts upon. Therefore, common daily activities such as people transit are dynamic loads. These must be considered in structural analysis to guarantee not only structural integrity and efficiency, but also user comfort.

That being stated, all dynamic analysis is based upon mathematical models that try to represent real systems as best as possible. How to construct and solve such models are the main concerns in dynamic analysis as these directly impact result precision and computational efforts.

Based on Jafari-Talookolaei, Abedi and Attar [1], in the construction of models many structures can be simplified as being two-dimensional (2D) without compromising most of the systems original properties. In the study of 2D elements, according to Zhou et al. [2], in plane vibrations are directly linked to energy transmission. Furthermore, as stated by Bercin and Langley [3], these gain significance as higher frequencies are analyzed. Different applications of in plane dynamic analysis can be found in works such as those proposed by Chen, Jin and Liu [4], Arreola-Lucas et al. [5], Wang et al. [6], Noori, Aslan and Temel [7] and Lyu et al. [8].

As for the solution, most mathematical models constructed to represent civil engineering structures do not have known analytical solutions and must be solved through approximated methods. Among these the Finite Element Method (FEM) is the most well established and widely used. Initially introduced in the 50's by Argyris [9] and Turner et al. [10], with the contributions of Clough [11], Melosh [12], Irons and Barlow [13] and Zienkiewicz and Taylor [14], among others, the method's main bases had already been fully established by the early 70's.

From this point onward the main focus of papers in the field became improving result precision and *h* and *p* refinement procedures were introduced by authors such as Oliveira [15] and Prager [16] respectively. While these refinements are implemented quite easily, they greatly increase the computational effort. In this context hierarchical methods, such as the Hierarchical Finite Element Method (HFEM) and Generalized Finite Element Method (GFEM) were created.

The GFEM incorporates known characteristics of the problem's differential equation solution into the approximated space. The method has been successfully applied to the dynamic analysis of different structures as can be seen, for example, in the works of Arndt, Machado and Scremin [17], Torii and Machado [18], Piedade Neto and Proença [19], Shang et al. [20] and Corrêa [21].

Although in comparison to traditional refinements the GFEM elevates convergence rates, it also increases the complexity of the numerical problem. According to Song et al. [22], as a way to counteract the increase in computational efforts, error estimators and indicators can be used to define which elements most affect the global solution. Once these are identified the enrichment may be locally applied and the numerical problem reduced. Among the different error indicators presented in previous literature, as compiled by Mackerle [23], the Friberg error indicator introduced by Friberg [24] has shown accurate results and has scarcely been applied to 2D dynamic analysis.

Therefore, the objective of this paper is to explore the use of the Friberg indicator as a guide to selective mesh enrichments. General characteristics and accuracy of the indicator were analyzed by comparing calculated eigenvalues to indicator values. All numerical results were obtained through coding in Python.

2 Finite element method

According to Zhao and Steven [25] in two-dimensional (2D) dynamic analysis two main types of problems may be evaluated: plane strain and plane stress problems. These simplifications can be found in a series of works such as Leung et al. [26], Kamal et al. [27] and Ho-Nguyen-Tan and Kim [28]. Considering such simplifications, if only free in plane vibration is analyzed and damping is neglected, a 2D dynamic problem is governed by:

$$\boldsymbol{L^T\sigma} - \rho\ddot{\boldsymbol{u}} = \boldsymbol{0}, \tag{1}$$

in which $\boldsymbol{L^T}$ is the matrix of differential operands:

$$\boldsymbol{L} = \begin{bmatrix} \frac{\partial}{\partial x} & 0 & \frac{\partial}{\partial y} \\ 0 & \frac{\partial}{\partial y} & \frac{\partial}{\partial x} \end{bmatrix}, \tag{2}$$

$\boldsymbol{\sigma}$ is the stress components vector, ρ is the material's specific mass and $\ddot{\boldsymbol{u}}$ is the acceleration vector relative to a 2D displacement field $\boldsymbol{u}$ with horizontal and vertical displacements u and v given by:

$$\boldsymbol{u} = [u \quad v]^T. \tag{3}$$

Neglecting damping effects in free vibration analysis is acceptable given that most common civil engineering structures have, as presented by Chopra [29], damping ratios below 20%. Small damping ratios lower natural frequencies and lengthen natural periods of vibration to approximately the same values as the undamped solution.

In accordance to Desai and Abel's [30] definition, the finite element method (FEM) is a numerical method through which a continuous system is approximated by a discrete system with a finite number of elements connected by nodal points. The behavior of each element is then obtained by a finite number of parameters. An assembly of all the elements leads to a global response that closely resembles that of the original continuous domain. The application of the Finite Element Method to Eq. (1) leads to the equation of motion:

$$\boldsymbol{M\ddot{u}} + \boldsymbol{Ku} = \boldsymbol{0}, \tag{4}$$

in which $\boldsymbol{M}$ and $\boldsymbol{K}$ are, respectively, the global mass and stiffness matrices. These are obtained through the assembly of the elementary mass and stiffness matrices:

$$\boldsymbol{M^e} = \int_V \rho \boldsymbol{N}^T \boldsymbol{N} dV, \tag{5}$$

$$\boldsymbol{K^e} = \int_V \boldsymbol{B}^T \boldsymbol{D} \boldsymbol{B} dV. \tag{6}$$

Equations (5) and (6) are formulated for an element with domain V. In these $\boldsymbol{N}$ is the matrix of shape functions, $\boldsymbol{B}$ is given by:

$$\boldsymbol{B} = \boldsymbol{LN} \tag{7}$$

and $\boldsymbol{D}$ is the material properties matrix. In the case of plane stress, as used in this paper, considering E as the elasticity modulus and ν as Poisson's ratio, $\mathbf{D}$ is given by:

$$\boldsymbol{D} = \frac{E}{1-\nu^2} \begin{bmatrix} 1 & \nu & 0 \\ \nu & 1 & 0 \\ 0 & 0 & (1-\nu)/2 \end{bmatrix}. \tag{8}$$

Details on the formulation presented until this point are presented in in Soriano [31]. Furthermore, considering the harmonic behavior of free vibration problems, Eq. (4), as detailed by Arndt [32], is a generalized eigenvalue and eigenvector problem given by:

$$\boldsymbol{Ku} - \omega^2 \boldsymbol{Mu} = \boldsymbol{0}. \tag{9}$$

2.1 Hierarchical shape functions

Gain in accuracy in FEM analysis is usually achieved through refinement procedures. As explained previously by Campion and Jarvis [33] the *p* refinement focuses on increasing the order of the functions used to describe the problem's variables. If standard *p* refinement is applied it requires that for every increase in function order a new group of functions be obtained. This greatly elevates computational costs as every term of the systems matrices needs to be recalculated. To avoid such problems hierarchical functions are used. When using hierarchical bases, shape functions of order *n+1* do not alter those of order *n*. This allows matrices of order *n* be submatrices of those with order *n+1*.

Two-dimensional hierarchical shape functions may be obtained by multiplying one-dimensional hierarchical shape functions (l), as presented by Torii [34]:

$$N_i = l_j(\xi) l_k(\eta). \tag{10}$$

In Eq. (10) N_i is a 2D shape function of a nodal point i referenced as j in the normalized ξ[-1,1] axis and as k in the normalized η[-1,1] axis. In this work these shape functions were obtained by the multiplication of Lobatto's one dimensional hierarchical polynomials. Lobatto's seven first original functions are represented in Fig. 1.

Equation (10) is valid considering the use of quadrilateral elements for the problem's discretization. This element's main drawbacks are that it restricts accurate geometry mapping and may lead to locking problems. However, it's simplicity greatly facilitates formulation of hierarchical and enriched elements, which, as previously stated, will be the focus of this research.

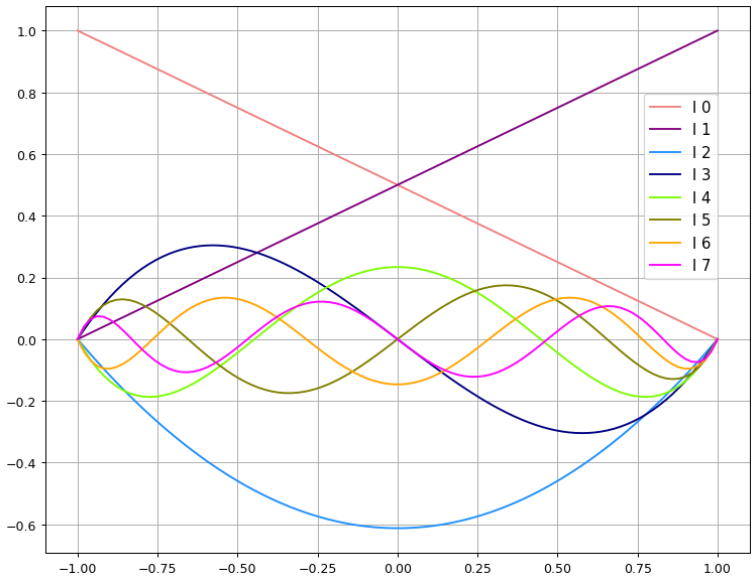

Figure 1. Lobatto's hierarchical polynomials

When working with 2D elements the increase in approximation order creates bubble and edge functions aside from the problem's original four nodal functions. Figure 2 represents the three types of functions mentioned.

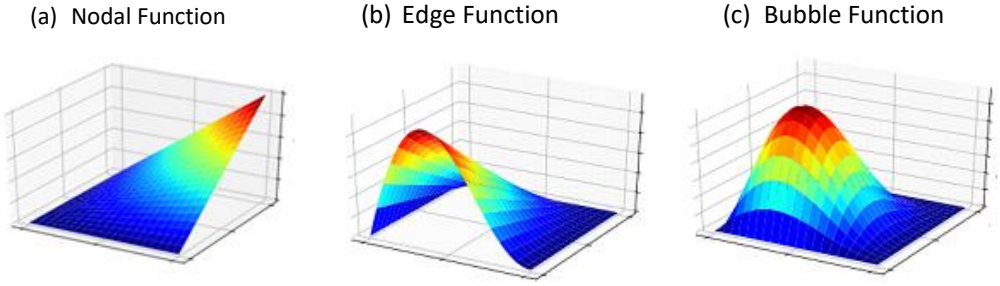

Figure 2. Types of hierarchical 2D functions

These functions may be independently inserted into de approximation. However, as presented by Solin [35], edge functions must be carefully treated once the conformity of adjacent elements must be maintained. Thus, as this work is the first step in a research that focuses on the accuracy of an error indicator and not, at the present time, in improving eigenvalue results, only bubble function will be used.

3 Generalized finite element method

According to Piedade Neto and Proença [19] the Generalized Finite Element Method (GFEM) consists in modifying basic partition of unity (PU) interpolation through enrichment functions. These are defined as functions with good approximation skills based on previous knowledge from known solutions. One of the main advantages of GFEM, in accordance with Shang et al. [20] is that it does not change the basic premises of classic FEM formulation, given that the used PU are conventional FEM functions.

Based on this, Arndt, Machado and Scremin [17] define the GFEM approximated solution u^e as:

$$u^e = u^e{}_{MEF} + u^e{}_{ENR}, \tag{11}$$

where $u^e{}_{MEF}$ is the classic FEM displacement field, and $u^e{}_{ENR}$ is the enriched displacement field. The enriched portion is, as exposed by Corrêa [21]:

$$u^e{}_{ENR} = \sum_{i=1}^{2} L_i \left(\sum_{j=1}^{nl} \Phi_{ij} a_{ij}\right), \tag{12}$$

where L_i are the PU functions, nl is the level of enrichment, Φ_{ij} are the enrichment base functions and a_{ij} the field (non-nodal) degrees of freedom.

In this paper the PU was taken as the Lagrangean linear functions and the enrichment base functions used were the trigonometric functions proposed by Arndt [32] and later modified by Torii [34]. These result in the following enriched shape functions written in a ξ [-1,1] domain:

$$\psi_{1j} = \frac{1-\xi}{2}\left[sin\left(\frac{\beta_j(\xi+1)}{2}\right)\right], \tag{13}$$

$$\psi_{2j} = \frac{1-\xi}{2}\left[cos\left(\frac{\beta_j(\xi+1)}{2}\right) - 1\right], \tag{14}$$

$$\psi_{3j} = \frac{1+\xi}{2}\left[sin\left(\frac{\beta_j(\xi-1)}{2}\right)\right], \tag{15}$$

$$\psi_{4j} = \frac{1+\xi}{2}\left[cos\left(\frac{\beta_j(\xi-1)}{2}\right) - 1\right], \tag{16}$$

where β_j is a parameter usually prescribed as $\beta_j = j\pi$. In this work $\beta_j = \pi$ will be used and the enriched functions can be seen in Fig. 3.

The construction of 2D enriched function follows the same process demonstrated in Section 2.1. Therefore, the same considerations made in regards to bubble and edge functions are valid in GFEM examples. Also, for the same reasons previously stated, this work will only apply bubble GFEM functions to enriched examples.

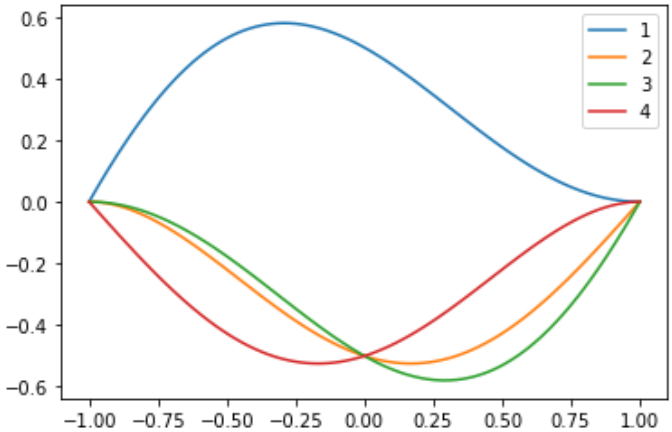

Figure 3. GFEM enriched 1D shape functions

4 Friberg error indicator

As presented by Song et al. [22] element shape, size and nodal point distribution are all factors directly linked to errors in discretization based approximated methods. Thus, the final error present in FEM and GFEM results can be seen as a sum of element error. In this context the importance of error indicators becomes clear, once these are capable of defining which elements have greater impact on the global solution. The application of higher levels of enrichments on such elements can greatly improve results with a computational cost lower than that obtained applying the enrichment on all elements.

In 1996 Friberg [24] proposed an error indicator that identifies the magnitude of eigenvalue variation in a hierarchical process. The indicator is mainly based on the Rayleigh quotient:

$$\lambda_i^{(n)} = \frac{\boldsymbol{\phi}_i^{(n)^T} \boldsymbol{K}_{(n)} \boldsymbol{\phi}_i^{(n)}}{\boldsymbol{\phi}_i^{(n)^T} \boldsymbol{M}_{(n)} \boldsymbol{\phi}_i^{(n)}}, \tag{17}$$

the measure of a specific frequency error e_i by:

$$e_i = \frac{\lambda_i^{(n)} - \lambda_i^{(n+m)}}{\lambda_i^{(n)}}, \tag{18}$$

with the representation of the problem's matrices in submatrices as exemplified:

$$\boldsymbol{K}_{(n+m)} = \begin{bmatrix} \boldsymbol{K}_{(n)} & \boldsymbol{K}_{(n,m)} \\ \boldsymbol{K}_{(m,n)} & \boldsymbol{K}_{(m)} \end{bmatrix}. \tag{19}$$

In Eq. (17) to (19) an original approximation of order n was hierarchically enhanced to order $n+m$. That being stated, $\boldsymbol{\phi}_i^{(n)}$ is the eigenvector associated with $\lambda_i^{(n)}$ eigenvalue of an approximation order n and $\lambda_i^{(n+m)}$ is the refined eigenvalue. Combining these principals, the Friberg indicator η_i is defined as:

$$\eta_i \approx \frac{\boldsymbol{\phi}_i^{(n)^T} \left[\boldsymbol{K}_{(m,n)} - \lambda_i^{(n)} \boldsymbol{M}_{(m,n)}\right]^T \left[\left[\boldsymbol{K}_{(m)} - \lambda_i^{(n)} \boldsymbol{M}_{(m)}\right]^{-1}\right]^T \left[\boldsymbol{K}_{(m,n)} - \lambda_i^{(n)} \boldsymbol{M}_{(m,n)}\right] \boldsymbol{\phi}_i^{(n)}}{\boldsymbol{\phi}_i^{(n)^T} \boldsymbol{K}_{(n)} \boldsymbol{\phi}_i^{(n)}}. \tag{20}$$

The detailed mathematical development of the indicator can be found in Friberg [24], Duarte [36] and Malacarne [37]. Equation (20) shows that the indicator does not depend on the $n+m$ problem's solution. However, the $n+m$ order matrices must still be calculated and for high order enrichments the indicator can demand high computational costs, especially due to the necessity of matrix inversion.

One of the ways to counteract the increase in computational effort as shown in Friberg [24], Friberg et al. [38] and Malacarne [37] is the use of the indicator's element sum property:

$$\eta_{total} = \sum_{i=1}^{k} \eta_i, \tag{21}$$

where a problem's Friberg indicator η_{total} can be obtained as the sum of each of its k elements individual η_i indicators. This property allows the reduction of the submatrices created by the enrichment process and, therefore, simplifies the indicator calculation.

Finally, it is important to note that the indicator is a dimensionless number that can assume negative values. In general, the higher the indicator value the greater is an element's effect on the global solution. Malacarne [37], showed that, for one-dimensional examples, even when negative values appeared the closest these were to positive numbers, the greater the element impact on result improvement. These correlations for two-dimensional analyzes have yet to be detailed.

5 Numerical results

With the intent of evaluating general characteristics of the Friberg indicator as well as it's accuracy both the indicator values and natural frequencies of in plane free vibrations were analyzed for different refinements. All examples considered the plane stress state. The analyzed structure, Fig. 4(a), was a square plate with dimensions $L = H = 1\ m$, thickness $t = 0.05\ m$, elasticity modulus $E = 210\ GPa$,

mass density $\rho = 8000\, kg/m^3$ and Poisson ratio $\nu = 0.3$. This same structure had been previously studied by Torii [34] and the author's results for highly refined HFEM simulations were used as reference.

Lobatto's first order polynomials were used for geometry mapping. Different meshes were used for numerical examples. All elements were numbered from bottom to top and right to left. All meshes will be referred to according to the number of rows and then columns. Figures 4(b), 4(c) and 4(d) respectively represent a 2x2, 3x3 and 5x5 mesh.

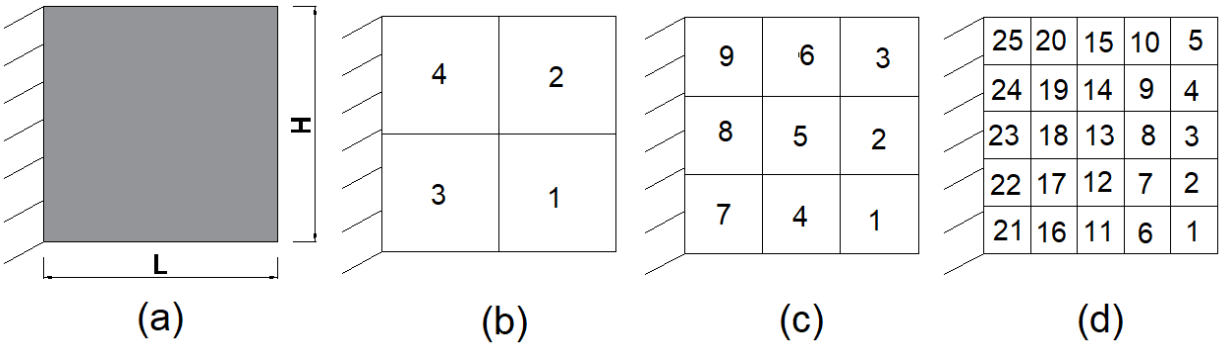

Figure 4. (a) Analyzed plate (b) 2x2 mesh (c) 3x3 mesh (d) 5x5 mesh

5.1 Indicator accuracy in HFEM

To determine the accuracy of the indicator all indicator values were calculated as well as all eigenvalues after the refinement was applied to each of the mesh's elements. Initially a single second order bubble function N_5:

$$N_5 = \left(\frac{1}{2}\sqrt{\frac{3}{2}}(\xi^2 - 1)\right) \times \left(\frac{1}{2}\sqrt{\frac{3}{2}}(\eta^2 - 1)\right), \tag{22}$$

was used in the refinement process. Tables 1 through 3 indicate the results obtained for different target frequencies and different meshes.

With the intent of facilitating visualization of the indicator accuracy all the tables are divided into four columns. The first and third columns contain, respectively, the remaining errors after the bubble function was added and the Friberg indicator values obtained. The second and fourth columns indicate which element was refined to obtain the results in the previous column. All results were ordered so that if the indicator correctly identifies the best refinement order, the second and fourth columns will be the same. All discrepancies observed were highlighted in yellow.

Based on the results shown in Tables 1 to 3 it can be stated that the Friberg indicator is capable of correctly identifying the best sequence in which to apply higher order functions selectively. The only exception to this behavior occurs when the refinement of different elements results in very similar errors.

This, however, can be attributed to possible numerical errors present in the analyses. Aside from that, it must be stated that the great proximity in calculated eigenvalues may be attributed to the symmetric characteristics of the analyzed structure and proposed meshes. Complex domains and distorted meshes will most likely lead to greater eigenvalue differences and, hence, indicator precision. Lastly, considering that rarely will a single element be refined, small discrepancies as observed will not affect final result precision.

Table 1. Results for the first frequency of a 3x3 mesh

Error after refinement (ascending)	Refined Element	Indicator value (descending)	Indicated Element
4.69%	7 or 9	0.006296074	7 or 9
4.95%	8	0.001622766	8
4.99%	5	0.000765749	5
5.01109%	1 or 3	0.000432685	4 or 6
5.01110%	4 or 6	0.000408973	3 or 1
5.03%	2	0.000099790	2

Table 2. Results for the twelfth frequency of a 3x3x mesh

Error after refinement (ascending)	Refined Element	Indicator value (descending)	Estimated Element
22.61%	2	0.031331997	2
23.88%	5	0.011536437	7 or 9
23.99%	7 or 9	0.009966959	5
24.34%	8	0.002720215	8
24.43%	4 or 6	0.001901176	4 or 6
24.47%	1 or 3	0.000986353	1 or 3

Table 3. Results for the sixth frequency of a 5x5 mesh

Error after refinement (ascending)	Refined Element	Indicator value (descending)	Indicated Element
3.830%	6 or 10	0.006572255	6 or 10
3.869%	11 or 15	0.006172690	11 or 15
3.984%	3	0.004092441	3
4.065%	12 or 14	0.002646015	12 or 14
4.065%	7 or 9	0.002621880	7 or 9
4.088%	2 or 4	0.002135207	2 or 4
4.111%	17 or 19	0.001798393	17 or 19
4.121%	1 or 5	0.001586163	1 or 5
4.124%	18	0.001560195	18
4.132%	16 or 20	0.001418959	16 or 20
4.171%	23	0.000731346	23
4.171%	8	0.000717640	8
4.187%	22 or 24	0.000426887	22 or 24
4.193%	13	0.000299469	13
4.198%	21 or 25	0.000219282	21 or 25

As previously stated in Section 4 the indicator is a dimensionless number that can assume negative values. These tend to be observed in the last frequencies of an approximation. Table 4 shows negative indicator results obtained for the analysis of the twenty-third frequency of a 3x3 mesh. For this case, since reference results were not available, the calculated frequencies were ordered in the first column in ascending order.

Table 4. Coefficients in constitutive relations

Calculated Frequency (rad/s)	Refined Element	Indicator value (descending)	Estimated Element
60005.72205	2	-0.113538647	8
60128.09292	5	-0.117485905	7 or 9
60298.08876	4 or 6	-0.369223106	5
60319.43695	8	-0.373628341	4 or 6
60354.98693	1 or 3	-0.682064403	2
60436.19543	7 or 9	-0.691384929	1 or 3

Contrary to the results obtained by Malacarne [37] for one-dimensional problems, it is shown in Table 4 that there is no direct relation between the best eigenvalue results and the absolute maximum indicator. Therefore, the negative Friberg indicator values are not recommended as parameters for defining the sequence of selective refinements. This does not pose a problem for most dynamic analysis given that negative values only appear on the last frequencies of an approximation which tend not to be the focus of most problems.

5.2 Indicator accuracy in GFEM

The same analysis previously demonstrated for HFEM was carried out in a GFEM problem to verify if the indicator behavior is the same. For this, sixteen enriched bubble functions were added to the classic FEM problem. These were obtained by multiplying the previously detailed functions shown in Fig. 3. The results for the first and the twelfth frequencies of a 3x3 mesh are presented in Tables 5 and 6. These are organized in the same way as previous tables.

Table 5. GFEM results for the first frequency of a 3x3 mesh

Error after refinement (ascending)	Refined Element	Indicator value (descending)	Estimated Element
4.67%	7 or 9	0.006594	7 or 9
4.94%	8	0.001701	8
4.99%	5	0.000808	5
5.0094%	1 or 3	0.000461	4 or 6
5.0095%	4 or 6	0.000435	1 or 3
5.03%	2	0.000111	2

Table 6. GFEM results for the twelfth frequency of a 3x3 mesh

Error after refinement (ascending)	Refined Element	Indicator value (descending)	Estimated Element
20.90%	2	0.062702	2
23.24%	5	0.021136	5
23.35%	1 or 3	0.020002	1 or 3
23.61%	4 or 6	0.016229	4 or 6
23.87%	7 or 9	0.014458	7 or 9
24.18%	8	0.005159	8

The results obtained reiterate the comments made in regards to HFEM. The Friberg indicator maintains the same precision in GFEM examples as it does in HFEM examples.

5.3 Simplifying the Friberg indicator calculation

The main concern related to the Friberg indicator is the computational effort associated with its calculation. This is especially due to the necessity of inverting a matrix which is a known demanding process. There are three main ways of reducing this problem, all of which reduce the order of the inverse matrix:

$$\left[\left[\boldsymbol{K}_{(m)} - \lambda_i^{(n)} \boldsymbol{M}_{(m)}\right]^{-1}\right]^T. \tag{23}$$

The first, as previously presented in Section 4 and indicated by Friberg [24], is the indicator's element sum property. This property states that if a refinement is applied to each of the mesh's individual elements, the sum of all the indicators will equal the value that would be obtained if the refinement was applied to all elements simultaneously. To test this, bubble function N_5 was applied individually and simultaneously to all four of a 2x2 mesh's elements in HFEM. The results can be seen in Table 7.

Table 7. Indicator element sum property

Frequencies	Simultaneous	Sum (1 + 2 + 3 + 4)
1	0.0259665	0.0259665
2	0.0335773	0.0335773
3	0.0998930	0.0998930
4	0.1016362	0.1016362
5	0.0837323	0.0837323
6	0.2761580	0.2761580
7	0.0384843	0.0384843
8	0.3854626	0.3854626
9	0.4473619	0.4473619
10	0.2233309	0.2233309
11	0.2233309	0.2233309
12	-1.6060391	-1.6060391

As expected, the results of both tests were the same. If a single new degree of freedom is introduced in a one-dimensional example, this characteristic automatically reduces the matrix presented in Eq. (23) to a single value, simplifying the mathematical procedure.

However, in 2D problems when the order of the approximation is elevated it affects two directions and, therefore, the minimum order of the matrix that must be inverted is two. Based on the same idea as the element sum procedure, this work tested the validity of dividing refinements in different directions.

A classic FEM approximation field in 2D analysis with the proposed quadrilateral element is made up of four shape functions ($N1, N2, N3, N4$) that result in a shape function matrix $\boldsymbol{N}$:

$$\boldsymbol{N} = \begin{bmatrix} N1 & 0 & N2 & 0 & N3 & 0 & N4 & 0 \\ 0 & N1 & 0 & N2 & 0 & N3 & 0 & N4 \end{bmatrix}. \tag{24}$$

If a single bubble function N_5 is added, as in previous tests, it will affect both the problem's horizontal direction (u) and vertical direction (v) and $\boldsymbol{N}$ will be defined as:

$$\boldsymbol{N} = \begin{bmatrix} N1 & 0 & N2 & 0 & N3 & 0 & N4 & 0 & N5 & 0 \\ 0 & N1 & 0 & N2 & 0 & N3 & 0 & N4 & 0 & N5 \end{bmatrix}. \tag{25}$$

What this work proposes is, therefore, dividing the problem into its directions by first refining the horizontal direction (u):

$$\boldsymbol{N} = \begin{bmatrix} N1 & 0 & N2 & 0 & N3 & 0 & N4 & 0 & N5 \\ 0 & N1 & 0 & N2 & 0 & N3 & 0 & N4 & 0 \end{bmatrix}, \tag{26}$$

and adding the resulting indicator value of an element with the result obtained by refining only the vertical direction (*v*) with:

$$\boldsymbol{N} = \begin{bmatrix} N1 & 0 & N2 & 0 & N3 & 0 & N4 & 0 & 0 \\ 0 & N1 & 0 & N2 & 0 & N3 & 0 & N4 & N5 \end{bmatrix}. \tag{27}$$

This procedure was carried out for all four elements of a 2x2 mesh and the results are presented in Table 8. The comparison of indicator results obtained by refining both directions simultaneously and by adding results of individually refining each direction were the same. This allows the reduction of the matrix in Eq. (23) to a single value for each individual calculation in a case were a *n* order problem is elevated to *n+1*.

Table 8. Indicator direction sum property

Element	Classic refinement	*u* refinement	*v* refinement	Sum of *u* and *v*
1	0.000946855	0.000792984	0.000153871	0.000946855
2	0.000946855	0.000792984	0.000153871	0.000946855
3	0.012036416	0.000118858	0.011917557	0.012036416
4	0.012036416	0.000118858	0.011917557	0.012036416

Up until this point all simplification procedures presented considered the elevation of a single degree of freedom in each of the problem's directions. However, most refinement procedures utilize a high number of new shape function and, hence, lead to a high number of field degrees of freedom. This implies that even if the element and direction sum properties are utilized, the matrices involved in the indicator calculation will still pose computational difficulties.

With the objective of always reducing the inverse matrix present in Eq. (23) to a single number, this work evaluated the possibility of applying shape functions consecutively instead of simultaneously for the indicator calculation. This example was analyzed through HFEM with the use of four of Lobatto's bubble shape functions:

$$N_5 = \left(\frac{1}{2}\sqrt{\frac{3}{2}}(\xi^2 - 1)\right) \times \left(\frac{1}{2}\sqrt{\frac{3}{2}}(\eta^2 - 1)\right), \tag{28}$$

$$N_6 = \left(\frac{1}{2}\sqrt{\frac{3}{2}}(\xi^2 - 1)\right) \times \left(\frac{1}{2}\sqrt{\frac{5}{2}}(\eta^2 - 1)\eta\right), \tag{29}$$

$$N_7 = \left(\frac{1}{2}\sqrt{\frac{5}{2}}(\xi^2 - 1)\xi\right) \times \left(\frac{1}{2}\sqrt{\frac{3}{2}}(\eta^2 - 1)\right), \tag{30}$$

$$N_8 = \left(\frac{1}{2}\sqrt{\frac{5}{2}}(\xi^2 - 1)\xi\right) \times \left(\frac{1}{2}\sqrt{\frac{5}{2}}(\eta^2 - 1)\eta\right). \tag{31}$$

The indicator values were calculated applying all four functions at once, the classic procedure, and by applying one after the other and adding up all the indicator results, the consecutive procedure. The comparison of each of these processes results considering the first frequency of a 3x3 mesh are shown in Table 9.

The results presented in Table 9 indicate that indicator results obtained through both procedures are very close in value but are not the same. These discrepancies may be caused by numerical errors. That being said, even though the results are not identical they indicate the same order of element priority. In conclusion, both procedures can be used to define which element has the greatest effect on the global solution.

Table 9. Consecutive refinement indicator values

Classic Procedure		Consecutive Procedure	
Indicator	Indicated Element	Indicator	Indicated Element
0.006481530	7 or 9	0.006493820	7 or 9
0.001672178	8	0.001673824	8
0.000794406	5	0.000796035	5
0.000452694	4 or 6	0.000454154	4 or 6
0.000427656	1 or 3	0.000430506	1 or 3
0.000108785	2	0.000108956	2

5.4 Friberg indicator as a global error estimator

Aside from indicating which elements mostly contribute to a global solution an ideal situation is that in which the indicator can be used as an error estimator. This means that the value of the indicator is able to represent the global error and based on this the obtained solution can be deemed as acceptable or not for a certain approximation. Friberg et al. [38] proposed using the sum of all of a refined mesh's indicators ${\eta_i}^{n+1}$ as a global error estimator ε according to:

$$\varepsilon = \sum {\eta_i}^{n+1} \quad for\ {\eta_i}^{n+1} > 0, \tag{32}$$

where all negative indicators are not considered.

To test the validity of the Friberg indicator as a global error estimator, HFEM function N5, used in previous examples, was added to all of the elements of different mesh discretizations. The final indicator value and the error of the first frequency in comparison to the reference value obtained by Torii [34] were calculated for each different discretization. These results are displayed in Fig. 5.

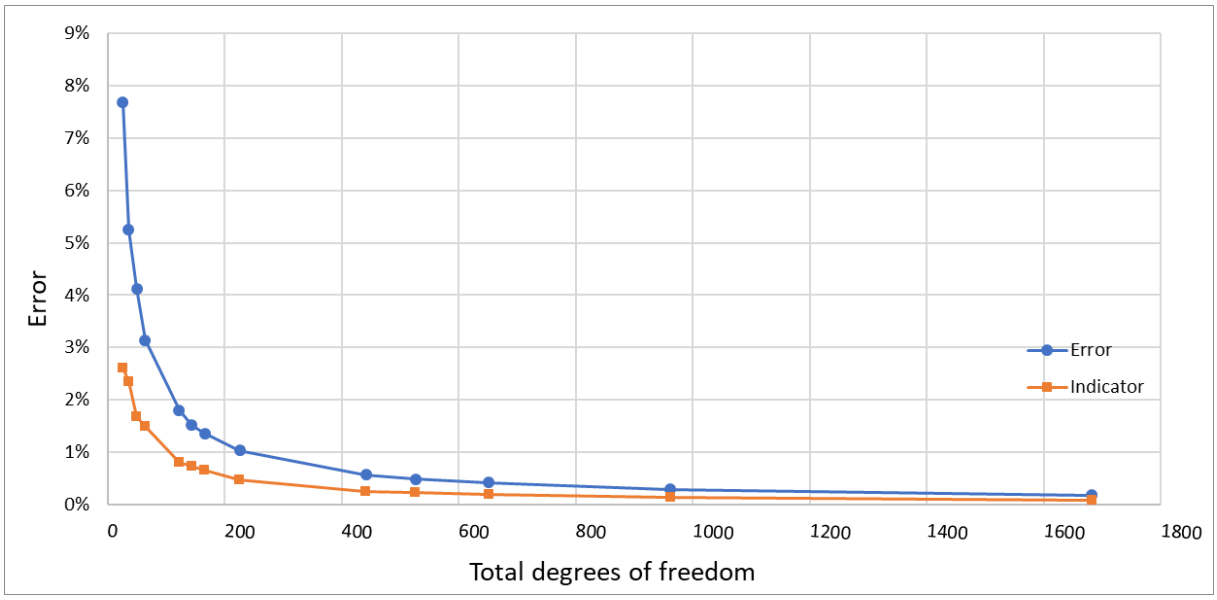

Figure 5. Error and indicator values for different meshes

It is clear that the indicator decreases as the global error decreases and both tend to zero as a greater number of elements is introduced in the mesh. However, the relation between the indicator and the error is not well defined as seen in Fig. 6. This means that knowing the indicator value cannot be trustfully

correlated with the error value. Therefore, the definition of a tolerance value that defines a small enough indicator to represent a desired error is subjective unless accompanied by a previous study of the error versus indicator variation for a specific problem and frequency.

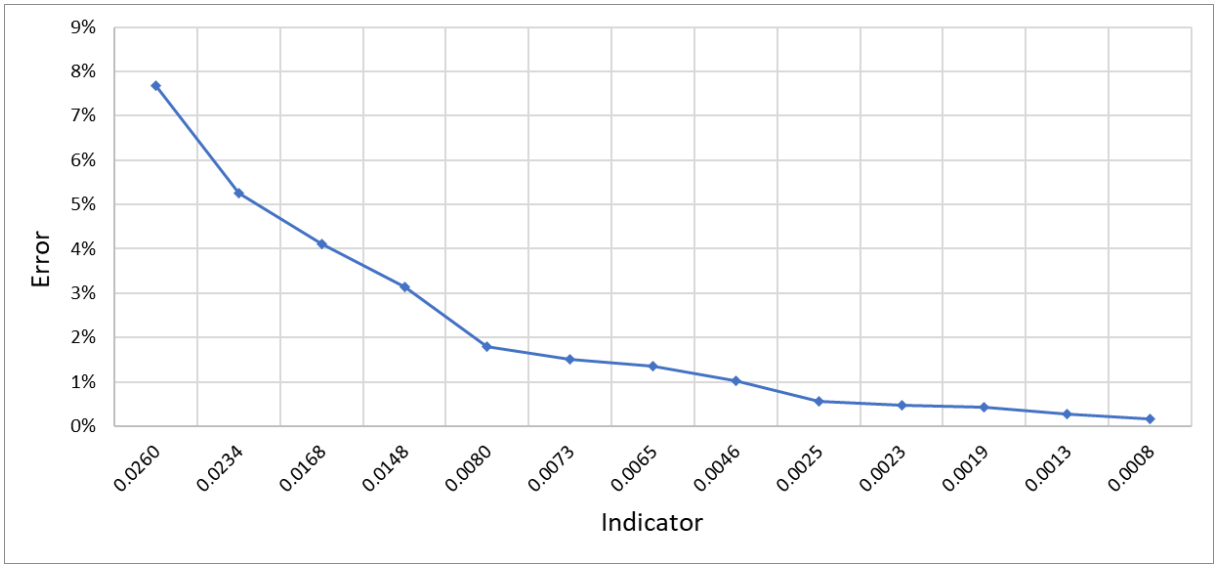

Figure 6. Error and indicator relation

6 Final remarks

Based on the examples presented in this work for HFEM and GFEM dynamic analysis it can be concluded that the Friberg indicator is an accurate measure for defining an element enrichment sequence in cases of selective enrichments. However, when used as a global error estimator a previous analysis of the indicator is recommended once it does not clearly relate to error values. Hence, tolerance values must be carefully chosen.

Finally, it was also shown that the necessity of inverting a matrix, which is a computationally demanding job, can be avoided with the use of the indicator's element and direction sum properties. In cases where higher levels of refinements are applied each shape function may be applied consecutively and lead to the same results as when applied simultaneously. It is important to note that even though this process reduces computational effort in obtaining each indicator value it requires that the process be repeated many times. Therefore, a detailed comparison of programming running times must be done to effectively determine if this process is advantageous.

It is expected that all behaviors observed are maintained in more complex geometries and boundary conditions as well as in cases of distorted meshes. Nevertheless, these cases must be analyzed in future works to confirm the indicator behavior.

Acknowledgements

The authors acknowledge CAPES and CNPq for the financial support.

References

[1] R. A. Jafari-Talookolaei, M. Abedi and M. Attar.In-plane vibration modes of laminated composite beams with arbitrary lay-ups. *Aerospace Science and Technology*, vol. 66, pp. 366–379, 2017.

[2] Y. Zhou, Q. Wang, D. Shing and Q. Liang. Exact solutions for the free in-plane vibrations of rectangular plates with arbitrary boundary conditions. *International Journal of Mechanical Sciences*, vol. 130, pp. 1-10, 2017.
[3] A. N. Bercin and R. S. Langley. Application of the dynamic stiffness technique to the in-plane vibrations of plate structures. *Computers & Structures*, vol. 59, n. 5, pp. 869-875, 1996.
[4] Y. Chen, G. Jin and Z. Liu. Flexural and in-plane vibration analysis of elastically restrained thin rectangular plate with cutout using Chebyshev-Lagrangian method. *International Journal of Mechanical Sciences*, vol. 89, pp. 264-278, 2014.
[5] A. Arreola-Lucas, J. A. Franco-Villafane, G. Báez and R. A. Méndez-Sánchez. In-plane vibrations of a rectangular plate: Plane wave expansion modeling and experiment. *Journal of Sound and Vibration*, vol. 342, pp. 168-176, 2015.
[6] Q. Wang, D. Shi, Q. Liang, Fazl and Ahad. A unified solution for free in-plane vibration of orthotropic circular, annular and sector plates with general boundary conditions. *Applied Mathematical Modelling*, vol. 40, n. 21-11, pp. 9228-9253, 2016.
[7] A. R. Noori, T. A. Aslan and B. Temel. An efficient approach for in-plane free and forced vibrations of axially functionally graded parabolic arches with nonuniform cross section. *Composite Structures*, vol. 200, pp. 701-710, 2018.
[8] P. Lyu, J. Du, Y. Wang and Z. Liu. Free in-plane vibration analysis of rotating annular panels with elastic boundary restraints. *Journal of Sound and Vibration*, vol. 439, pp. 434-456, 2018.
[9] J. H. Argyris. Energy Theorems and Structural Analysis: A Generalized Discourse with Applications on Energy Principles of Structural Analysis Including the Effects of Temperature and Non-Linear Stress-Strain Relations. *Aircraft Engineering and Aerospace Technology*. vol. 26, n. 10, pp.347-356, 1954.
[10] M. J. Turner, R. W. Clough, H. C. Martin and L. J. Topp. Stiffness and Deflection Analysis of Complex Structures. *Journal of the Aeronautical Sciences*, vol. 23, n. 9, pp. 805-824, 1956.
[11] R. W. Clough, 1960. The Finite Element Method, in Pane Stress Analysis. *Proc. 2nd A.S.C.E. Conf. on Electronic Comp*.
[12] R. J. Melosh. Basis for Derivation of Matrices for the Direct Stiffness Method. *AIAA Journal*, vol. 1, n. 7, pp. 1631-1637, 1963.
[13] B. Irons and J. Barlow. Comment on Matrices for the Direct Stiffness Method. *AIAA Journal*, vol. 2, n. 2, pp. 403-404, 1964.
[14] O. C. Zienkiewicz and R. L. Taylor. *The Finite Element Method. 5. ed*. Elsevier Butterworth-Heinemann, 2000.
[15] E. R. A. Oliveira. Theoretical foundations of the finite element method. *International Journal of Solids and Structures*, vol. 4, n.10, pp. 929-952, 1968.
[16] W. Prager. A note on the optimal choice of finite element grids. *Computer Methods in Applied Mechanics and Engineering*, vol. 6, pp. 363-366, 1975.
[17] M. Arndt, R. D. Machado, A. Scremin. Accurate assessment of natural frequencies for uniform and non-uniform Euler-Bernoulli beams and frames by adaptive generalized finite element method. *Engineering Computations*, vol. 33, n. 5, pp. 1586-1609, 2016.
[18] A. J. Torii and R. D. Machado. Structural dynamic analysis for time response of bars and trusses using the generalized finite element method. *Latin American Journal of Solids and Structures*, vol. 9, n. 3 pp. 1-31, 2012.
[19] D. Piedade Neto, S. P. B. Proença. Generalized Finite Element Method in linear and nonlinear structural dynamic analyses. *Engineering Computations*, vol. 33, n. 3, pp. 806-830, 2016.
[20] H. Y. Shang, R. D. Machado and J. E. Abdalla Filho and M. Arndt. Numerical analysis of plane stress free vibration in severely distorted mesh by Generalized Finite Element Method. *European Journal of Mechanics/A Solids*, vol. 62, pp. 50-66, 2017.
[21] R. M. Corrêa. Análise dinâmica de arcos utilizando o Método dos Elementos Finitos Generalizados. Masters Dissetation, Universidade Federal do Paraná, 2019.
[22] C. Song, E. T. Ooi, A. L. N. Pramod and S. Natarajan. A novel error indicator and an adaptive refinement technique using the scaled boundary finite element method. *Engineering Analysis with Boundary Elements*, vol. 94, pp. 10-24, 2018.
[23] J. Mackerle. Error estimates and adaptive finite element methods: A bibliography (1990-2000). *Engineering Computations*, vol. 18, n. 5-6, pp. 802-914, 2001.

[24] P. O. Friberg. An error indicator for the generalized eigenvalue problem using the hierarchical finite element method. *International Journal for Numerical Methods in Engineering*, vol. 23, pp. 91-98, 1986.
[25] C. Zhao, G. P. Steven. Asymptotic Solutions for Predicted Natural Frequencies of Two-Dimensional Elastic Solid Vibration Problems in Finite Element Analysis. *International Journal for Numerical Methods in Engineering*, vol. 39, pp. 2821-2835, 1996.
[26] A. Y. T. Leung, B. Zhu, J. Zheng and H. Yang. Analytic trapezoidal Fourier p-element for vibrating plane problems. *Journal of Sound and Vibration*, vol. 271, pp. 67-81, 2004.
[27] S. M. Kamal, U. S. Dixit, A. Roy, Q. Liu and V. V. Silberschimidt. Comparison of plane-stress, generalized-plane-strain and 3D FEM elastic–plastic analyses of thick-walled cylinders subjected to radial thermal gradient. *International Journal of Mechanical Sciences*, vol. 131-132. pp. 744-752, 2017.
[28] T. Ho-Nguyen-Tan, H. Kim. An interface shell element for coupling non-matching quadrilateral shell meshes. *Computers and Structures*, vol. 208, pp. 151-173, 2018.
[29] A. K. Chopra. *Dynamics of Structures: Theory and Applications to Earthquake Engineering*, 3. ed. Prentice Hall, 1995.
[30] C. S. Desai and J. F. Abel. *Introduction to the finite element method.* Van Nostrand Reinhold Company, 1972.
[31] H. L. Soriano. *Elementos Finitos: Formulação e Aplicação na Estática e Dinâmica das Estruturas.* Ciência Moderna, 2009.
[32] M. Arndt. O Método dos elementos finitos generalizados aplicado à análise de vibrações livres de estruturas reticuladas. Doctor thesis, Universidade Federal do Paraná, Curitiba, 2009.
[33] S. D. Campion and J. L. Jarvis. An investigation of the implementation of the p-version finite element method. *Finite Elements in Analysis and Design*, vol. 23, pp. 1-21, 1996.
[34] A. J. Torii. Análise dinâmica de estruturas com o método dos elementos finitos gerenalizado. Masters dissertation, Universidade Federal do Paraná, 2012.
[35] P. Solin, K. Segeth and I. Dolezel. *Higher-Order Finite Element Methods*. Chapman & Hall/CRC, 2004.
[36] H. V. Duarte. Estimador de Erro para a Formulação p do Método dos Elementos Finitos Aplicado ao Problema Fluido-Estrutura. Doctor thesis, Universidade Estadual de Campinas, 2003.
[37] M. F. Malacarne. O indicador de erro de Friberg empregado no método dos elementos finitos generalizados aplicado à análise dinâmica de estruturas. Masters dissertation, Universidade Federal do Paraná, 2018.
[38] P. O. Friberg, P. Moller, D. Makovicka and N. E. Wiberg. An adaptive procedure for eigenvalue problems using the hierarchical finite element method. *International Journal for Numerical Methods in Engineering*, vol. 24, pp. 319-335, 1987.